

Supplemental Information

Sequential ATP Hydrolysis and Interlaced Nucleotide Exchange is Preserved at Low [ATP].

Packaging trajectories of WT motors at very low ATP ([ATP]=20 μ M) in the presence of small amounts of ATP γ S (500:1 molecular ratio, i.e. in 100 motor cycles one of the 5 subunit is likely to bind ATP γ S) exhibited the distinct pauses previously observed at saturating [ATP] (1). The duration of these pauses is single exponentially-distributed showing that a single event defines the duration of the pause (Fig. S1a). The pause density increases linearly with [ATP γ S] (the highest [ATP γ S] tested was 125:1 molecular ratio, meaning that in 25 motor cycles one of the 5 subunits is likely to bind ATP γ S), suggesting that a single molecule is enough to halt the motor (Fig. S1a). The pause duration does not change with [ATP γ S], consistent with a mechanism in which the residence time of a single ATP γ S molecule in the subunit defines the duration of the pause (Fig. S1a). Previously, it was shown that at saturating [ATP] the hydrolysis events are strictly sequential, and as result, binding of a single ATP γ S molecule is enough to interrupt the catalytic phase (1). These results show that one ATP γ S molecule is also enough to halt the motor at limiting [ATP], implying that sequential ATP hydrolysis continues to take place in these limiting conditions. We conclude that the subunits' coordination during the catalytic phase is preserved even when the ring is not fully saturated with ATP.

Additionally, a careful ATP titration at sub K_m [ATP] shows that the motor's velocity is best described by the Hill equation with the coefficient, $n_H=1$ (Fig. S1b). This result could be interpreted simply as lack of cooperative binding (2). However, we previously showed that a scheme of sequential ATP binding at saturating [ATP] exhibits the binding dynamics of a single enzyme (or $n_H=1$) since at any given time only one pocket is available to bind the nucleotide (3). Thus, we conclude that ATP binding continues to take place sequentially at low [ATP]. Moreover, competition experiments with ADP show that the mean dwell duration increases linearly as a function of [ADP] (Fig. S1b). Such linear behavior is in agreement with the competitive ADP inhibition observed at saturating [ATP] (Fig. S1c). Competitive ADP inhibition within a sequential ATP binding scheme is only possible if the ADP release events and the ATP binding events are interlaced—see (1) for alternative scenarios. We conclude that coordination during nucleotide exchange is preserved at limiting [ATP].

Analysis of the Bi-Modal Population in R146A/WT Mixtures. In R146A/WT mixing experiments, a 1:4 (R146A:WT) or 20% mutant mixing condition yielded two phenotypes: slow (\sim 10 bp/s) and WT-like behavior (\sim 125 bp/s), whereas a 1:3 (R146A:WT) or 25% mixing condition yielded only the slow packaging behavior. In both conditions, we either got active tethers or no tethers. The slow packaging behavior displayed consistently 10 bp bursts, suggesting that 4 subunits—each capable of powering 2.5 bp of DNA translocation (3)—are competent for DNA translocation and hydrolysis. Thus, we continue to analyze the binomial velocity distributions assuming that ring motors with two or more mutant subunits in the ring are inactive, and that mutant subunits have equal probability to be incorporated in the ring as WT subunits. The latter is a reasonable assumption given that 1) motor subunits bind to a pRNA scaffold to form the ring configuration, 2) the pRNA binding site in the subunit is far from the residue mutated, R146 and 3) the pRNA-subunit binding is not affected by the presence of nucleotide, ATP or AMP-PNP (4). The proportion of molecules with slow

packaging behavior suggest that rings with one mutant subunit at any position can support packaging with 10 bp bursts. Indeed, we have previously shown that rings with a temporarily inactive translocating subunit (by the binding of ATP γ S) are able to resume packaging activity after subunit reassignment, such that the inactivated subunit adopts the regulatory role (1). Because, we observe only 10 bp bursts, and not 7.5, 5 or 2.5 bp bursts which would evidence an inactive translocating subunit, we conclude that the inactive subunit must have taken on the regulatory role early on at the pre-packaging stage in solution. In fact, the slight discrepancy between the predicted number of ring motors containing a single mutant (55%) and the observed number of slow motors (45%) could be due to failure of subunit reassignment leading to non-processive motors. In the 25% mutant condition, the bimodal distribution predicts that a 37% corresponds to WT rings and 63% to rings with a single mutant. In the experiment, all tethers (7 molecules) displayed the slow packaging behavior. We attribute the lack of tethers with WT-behavior to the low number of events and the fact that mixture samples were allowed to pre-package 30 s longer than WT samples before stalling the viral complexes. This extra time was necessary to favor the packaging initiation of the slower mutant rings, but in turn, it allowed WT motors (packaging rate at \sim 125 bp/s) to package \sim 3.7 kb of DNA. In WT samples, motors are often tethered as they are packaging the last 3 kb piece of DNA. Thus, it is likely that a fraction of WT-like motors in the mixture samples had already completed packaging by the time the motors could be tethered.

Estimated Population Fractions for Various Numbers of R146K Mutants Tolerated in the Ring. In the R146K/WT mixing experiments, the motors' velocity clustered roughly in three main groups: fast (\sim 125 bp/s, WT-like), intermediate (\sim 85 bp/s) and slow (\sim 45 bp/s) (Fig. 3b). This observation rules out the simplest scenario in which the motor can tolerate only 1 mutant subunit, displaying the same phenotype whether it affects a translocating or the non-translocating subunit, for in that case only two populations (WT and slower motors) would be observed. Next, we considered the case in which a single mutant subunit is tolerated in the ring but affects differentially the translocating and the non-translocating subunits, a scenario that would explain the three peaks observed. In this case, we would expect that as the ratio of mutant-to-WT subunits is increased in the mixture, the heights of the two slower peaks should grow at the expense of the WT peak but their relative proportion should not change. However, the results in Fig. 3b indicate that the size of the two slower populations change relative to one another, clearly ruling out also this scenario. Therefore, we conclude that the motor can tolerate 2 or more R146K subunits. This conclusion was verified in the following quantitative analysis: for each mixing condition (0%, 25%, 33% or 40%), each group (cluster) was fitted to a Gaussian distribution (Fig. 3b). The superposition of the Gaussian functions within one mixing condition was normalized. The area under each Gaussian was considered to be the fraction of motors belonging to either group (WT-Like, intermediate or slow) in a given mixing condition. Next, we proceeded to estimate the fractions of ring motors with 1, 2, 3 and 4 R146K subunits predicted by the binomial distribution and by the four R146K/WT mixing ratios (0%, 25%, 33% and 40% of the subunits were R146K), assuming that either subunit, mutant or WT, has the same affinity to be incorporated in the ring (see argument in previous section). Next, we considered individually the scenarios of allowing the motor to tolerate up to 1, 2, 3 or 4 R146K subunits. In each

scenario, motors with more mutant subunits than the maximum allowed were considered inactive, and the fractions were normalized after discarding the portion of inactive motors for each scenario (see Sup. Table 1). We observed that, in all mixing conditions the estimated number of WT motors (0 mutant subunits in the ring) was higher compared to the fraction of WT-like traces observed experimentally (Fig. 3b). We rationalize this observation considering that a fraction of WT-like motors in the mixture samples is likely to have already completed packaging by the time the motors could be tethered (see argument in previous section). We next proceeded to assign the slow and intermediate groups to rings with different number of mutants, or a combination of them, accordingly to the maximum number of mutant subunits tolerated in each scenario. In the scenario where rings tolerate only 1 mutant subunit (case a), we assigned the slow group to rings with 1 mutant non-translocating subunit, and the intermediate group to rings with 1 mutant translocating subunit (see Sup. Table 1). In scenarios where rings could tolerate up to 2 (case b), 3 (case c) or 4 (case d) R146K mutants in the ring, the intermediate group was assigned to rings with 1 mutant subunit in case b, and the superposition of rings with 1 and 2 mutant subunits in cases c and d (see Sup. Table 1). Similarly, the slow group was assigned to rings with 2 mutants in case b, 3 mutants in case c and 3 and 4 mutants in case d. With these assignments we obtained for each case an estimated fraction of motors in each group (WT-like, intermediate and slow) for each mixing condition. Next, we estimated the *goodness* of each case by measuring the *variance* relative to the experimental distribution. The *variance* for a given case x is defined as follows:

$$Var_x = \sum_{i,j} (F_{Tij} - F_{Eij})^2$$

Where F_{Tij} is the estimated fraction of group i in the mixing condition j , and F_{Eij} is the experimental fraction of group i in the mixing condition j . As shown by the *variance* value, the estimated fractions were closer to the experimental ones in cases c and d. Thus, according to this analysis then, rings can tolerate 3 or more R146K subunits without complete loss of packaging activity.

Derivation of an Analytical Expression for the Motor's Packaging Velocity. The packaging velocity is the ratio of the length of DNA packaged per translocation event (10 bp) to the total duration of the motor's cycle. The latter is the inverse of the cycle rate, k_{cycle} , which depends on the rate at which the motor completes nucleotide exchange and hydrolysis and phosphate release in *all* 5 (4 translocating and 1 non-translocating) subunits, $k_{nuc,cycle}$ and $k_{h,cycle}$, respectively. The rate for the overall k_{cycle} can then be written as:

$$k_{cycle} = \frac{k_{nuc,cycle} \cdot k_{h,cycle}}{k_{nuc,cycle} + k_{h,cycle}} \quad (5)$$

Here, $k_{h,cycle} = k_h/5$, with k_h being the rate of hydrolysis and phosphate release rate per subunit. Initially, we neglected the difference in these parameters between the non-translocating and translocating subunits. It was previously showed that nucleotide exchange takes place sequentially, one subunit at a time (1). Moreover, the kinetic events of nucleotide exchange in each subunit are

$$v = \frac{\frac{V_{nucx}}{V_{nucx} \cdot \left(\frac{1}{k_{h,cycle}}\right) + 4} * [ATP]}{[ATP] + \frac{K_{nucx}}{V_{nucx} \cdot \left(\frac{1}{4 \cdot k_{h,cycle}}\right) + 1}} * 10bp \quad (8)$$

Since the rate of the catalytic phase is faster ($k_{h,cycle}$ is $\sim 100 \text{ s}^{-1}$ based on the mean burst duration $\sim 0.01 \text{ s}$) than the rate of ADP release per subunit (k_{ADPr} is $\sim 50 \text{ s}^{-1}$ assuming 4 ADP release events during a mean dwell duration $\sim 0.072 \text{ s}$, see Monte Carlo simulation below), and therefore, $4k_{h,cycle} \gg k_{ADPr}$, it can be shown that $4k_{h,cycle} \gg V_{nucx}$, and thus the overall velocity of the cycle can be approximated as:

$$v = \frac{V_{cycle} * [ATP]}{[ATP] + K_{cycle}} * 10bp$$

where

$$V_{cycle} \approx \frac{V_{nucx}}{4} = \frac{k_{ADPr}}{4 \cdot \left(1 + \frac{k_{ADPr}}{k_{ATP_tight}}\right)} \quad (9)$$

and

$$K_{cycle} \approx K_{nucx} = \frac{k_{ADPr} \cdot \left(1 + \frac{k_{ADPr}}{k_{ATP_tight}}\right)}{k_{ATPb} \cdot \left(1 + \frac{k_{ADPr}}{k_{ATP_tight}}\right)} \quad (10)$$

The contribution of $k_{h,cycle}$ to V_{cycle} and K_{cycle} is only about 10% in Eq. 9 and 10. In the analysis of R146K/WT hybrid motors in ADP competition experiments, V_{cycle} and K_{cycle} is referred to as V_{max} and K_m , respectively.

Monte-Carlo Simulation of the Motor's Mechano-Chemical Cycle and its Inhibition by ADP. The Monte Carlo algorithm uses the kinetic scheme (5) of the previous section to compute the duration of each cycle, assuming that all 5 subunits of the ring must exchange nucleotide sequentially one subunit at a time. The 5 subunits must bind ATP before the first hydrolysis event is allowed, and the catalytic phase is coupled to a 10 bp translocation event. The cycle is repeated 1000 times (equivalent to packaging 10 kb). The packaging velocity is estimated as the amount of packaged DNA over the total time it takes to complete the 1000 cycles. The kinetic parameters that reproduced the behavior of WT motors at saturating [ATP] conditions (500 μM) are: $k_{ATPb} = 1.1 \mu\text{M}^{-1} \text{ s}^{-1}$, $k_{ATPr} = 50 \text{ s}^{-1}$, $k_{ADPr} = 50 \text{ s}^{-1}$, $k_{ATP_tight} = 5000 \text{ s}^{-1}$, $k_{h,cycle} = 10 \text{ s}^{-1}$. The amount of ADP inhibition observed in WT motors ([ADP]=500 μM) is well reproduced by the following kinetic rate: $k_{ADPb} = 0.5 \mu\text{M}^{-1} \text{ s}^{-1}$. According to Eq. 9, a reduction in V_{max} must derive from changes in k_{ADPr} and/or k_{ATP_tight} . Maintaining other rates equal, the following reduction in kinetic rates reproduced the velocity of F145I rings ($\sim 65 \text{ bp/s}$): i)

$k_{ATP_tight} = 50 \text{ s}^{-1}$ alone or ii) $k_{ADPr} = 23 \text{ s}^{-1}$ alone, and the slowest population in the R146K/WT mixtures ($\sim 45 \text{ bp/s}$): i) $k_{ATP_tight} = 18 \text{ s}^{-1}$ alone or ii) $k_{ADPr} = 12 \text{ s}^{-1}$ alone. In either case, reducing simultaneously both rates resulted in the same behavior as reducing only k_{ADPr} . According to Eq. 10, for K_m to remain invariant, a reduction in k_{ADPr} must be accompanied by the proportional change in k_{ATPb} . Thus, the following rate constants reproduced the velocity and K_m values of F145I rings: $k_{ADPr}=23 \text{ s}^{-1}$ and $k_{ATPb}=0.69 \text{ }\mu\text{M}^{-1} \text{ s}^{-1}$, and of R146K/WT hybrid rings: $k_{ADPr}=12 \text{ s}^{-1}$ and $k_{ATPb}=0.36 \text{ }\mu\text{M}^{-1} \text{ s}^{-1}$. Table S2 summarizes the results of this simulation.

References in Supplemental Information

1. Chistol G, Liu S, Hetherington CL, Moffitt JR, Grimes S, Jardine PJ, et al. High degree of coordination and division of labor among subunits in a homomeric ring ATPase. Cell [Internet]. Elsevier Inc.; 2012 Dec 21 [cited 2014 Jan 31];151(5):1017–28. Available from: <http://www.pubmedcentral.nih.gov/articlerender.fcgi?artid=3652982&tool=pmcentrez&rendertype=abstract>
2. Copeland R a. Cooperativity in Enzyme Catalysis. In: Enzymes [Internet]. 2002. p. 367–84. Available from: <http://dx.doi.org/10.1002/0471220639.ch12>
3. Moffitt JR, Chemla YR, Aathavan K, Grimes S, Jardine PJ, Anderson DL, et al. Intersubunit coordination in a homomeric ring ATPase. Nature [Internet]. 2009 Jan 22 [cited 2014 Jan 31];457(7228):446–50. Available from: <http://www.pubmedcentral.nih.gov/articlerender.fcgi?artid=2716090&tool=pmcentrez&rendertype=abstract>
4. Ding F, Lu CR, Zhao W, Rajashankar KR, Anderson DL, Jardine PJ, et al. Structure and assembly of the essential RNA ring component of a viral DNA packaging motor. Proc Natl Acad Sci U S A. 2011;108(18):7357–62.
5. Moffitt JR, Bustamante C. Extracting signal from noise: kinetic mechanisms from a Michaelis-Menten-like expression for enzymatic fluctuations. FEBS J [Internet]. 2014 Jan [cited 2014 Jan 29];281(2):498–517. Available from: <http://www.ncbi.nlm.nih.gov/pubmed/24428386>

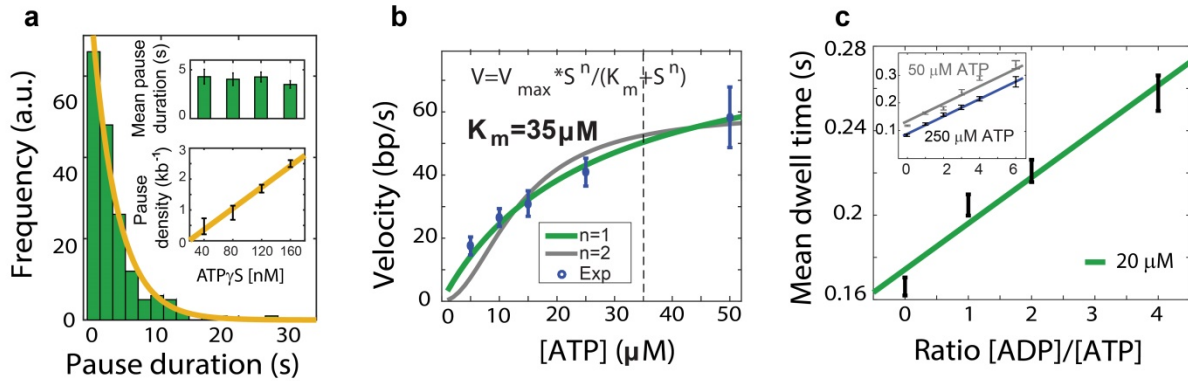


Figure S1. Coordination is preserved at low [ATP]. a) Analysis of pauses induced by the non-hydrolyzable ATP analog, ATP γ S. [ATP]= 20 μM . b) ATP titration below K_m conditions. Packaging velocity as a function of [ATP] fits well to the hill equation with coefficient $N_H=1$. c) ADP inhibition at low [ATP] ([ATP]=20 μM).

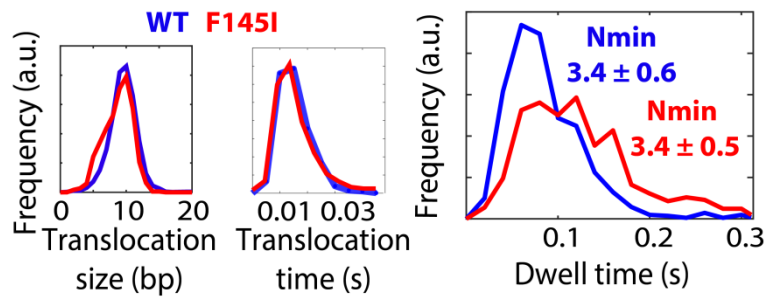


Figure S2. High-resolution analysis of F145I and WT homomeric ring motors. Left, size and duration of translocation events. Left, analysis of dwell times. N_{\min} (defined as $\langle \tau \rangle^2 / (\langle \tau^2 \rangle - \langle \tau \rangle^2)$, where τ is the dwell time) is a statistical parameter that reflects the lower bound to the number of rate-limiting events in a given process.

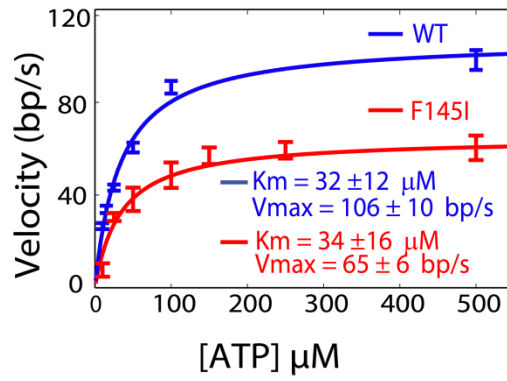


Figure S3. Michaelis-Menten parameters of F145I and WT ring motors. Multiple packaging trajectories were collected at different [ATP] conditions. For any given [ATP] condition, the data represents the mean packaging velocity of multiple trajectories in that condition. Error bars reflect the standard error of the mean.

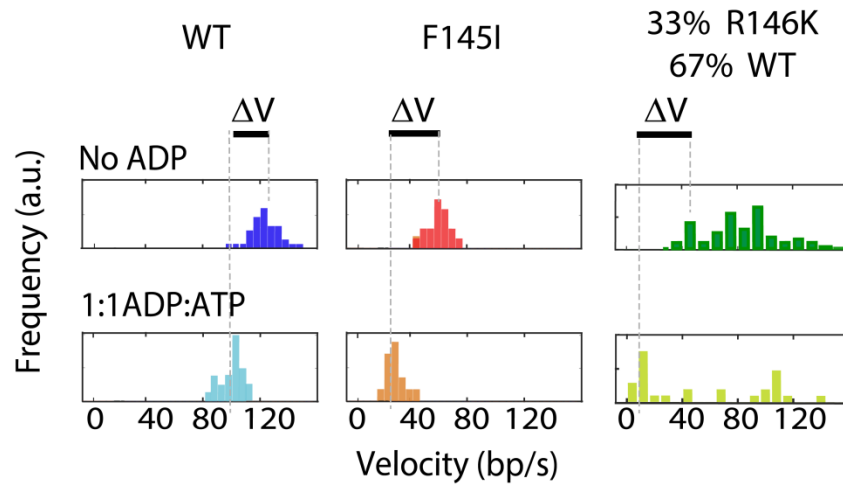


Figure S4. Analysis of ADP inhibition of WT and mutant packaging motors. Homomeric WT (blue) and F145I rings (red) and of the slowest population of R146K/WT hybrid rings (green). Dashed lines represent mean values of the whole distribution in WT and F145I, and mean values of the slowest group in R146K/WT ring motors. The slowest group was determined through a Gaussian fit as described in Supplemental Information.

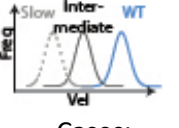
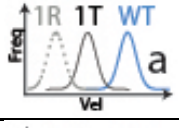
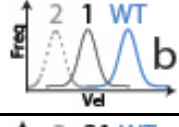
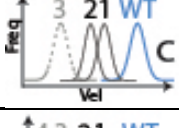
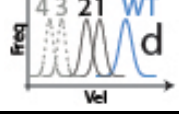
 Cases:	Population fractions for 1:3 mixing ratio – (25%)			Population fractions for 1:2 mixing ratio – (33%)			Population fractions for 2:3 mixing ratio – (40%)			Variance (deviation from experiment)
	WT-like	Inter-mediate	Slow	WT-like	Inter-mediate	Slow	WT-like	Inter-mediate	Slow	
Experimental	0.09	0.78	0.128	0.09	0.78	0.13	0	0.6	0.39	0
 a	0.37	0.5	0.125	0.29	0.57	0.14	0.23	0.61	0.15	0.35
 b	0.26	0.44	0.26	0.16	0.41	0.41	0.11	0.37	0.5	0.45
 c	0.24	0.67	0.08	0.16	0.69	0.14	0.085	0.66	0.25	0.08
 d	0.23	0.65	0.1	0.2	0.66	0.13	0.07	0.61	0.31	0.07

Table S1. Estimated population fractions for rings tolerating various numbers of R146K mutant subunits.

Compare cases across rows. Experimental: fractions were obtained as the area under the Gaussian fit for each group. Case a, b, c and d: fractions were calculated based on the binomial distribution and the mixing ratio (1:3, 1:2 or 2:3). Case a: the ring tolerates 1 mutant subunit, but the substitution affects differentially the translocating and regulatory subunits. In the schematic velocity distribution (first column), 1R refers to 1 mutant regulatory subunit and 1T to 1 mutant translocating subunit. Case b, c and d: the ring tolerates a maximum of 2, 3 and 4 mutants in the ring, respectively. In the schematic velocity distributions (first column): 1 = rings with one mutant subunit, 2 = rings with 2 mutant subunits, 3 = rings with 3 mutant subunits and 4 = rings with 4 mutant subunits.

	WT scenario		F145I - 5 mutant subunits				R146K/WT- 3* mutant subunits in the ring			
	Exp. data	M.C.	Exp. data	k_{ATP_tight} 1/50	k_{ADPr} 1/23	$k_{ADPr} - 1/23$ $k_{ATPb} - 0.69$	Exp. data	k_{ATP_tight} 1/18	k_{ADPr} 1/12	$k_{ADPr} - 1/12$ $k_{ATPb} - 0.36$
V_{max}	125	128	65	64.5	66.5	65.5	45	45.5	46.5	45.5
K_m	32	33.5	35	31	18.5	37	N/M	--	--	--
N_{min}	3.4	3.6	3.5	7.2	3.7	3.3	N/M	--	--	--
$V_{ADP_1:1}$	105	103	30	50.5	52	36	15	35.5	37.5	18
% ΔV	16%	19.5%	54%	22%	22%	45%	67%	22%	19%	60.5%

Table S2. Summary of results of Monte-Carlo simulation.

Compare across columns. In the WT scenario, experimental values are displayed in green. The rate constants in the Monte Carlo (M.C.) simulation were selected to match the experimental values, starting from previous values (Chistol et al., 2012). See Extended Experimental Procedure for all rate constants. In the F145I and R146K/WT scenarios, the modified rate constants (indicated in the top of each column) were selected to match the experimental velocity corresponding to either case (shown in green). The remaining rate constants were kept as in the WT scenario. $V_{ADP_1:1}$ is the velocity of the motor in the presence of equal amounts of ATP and ADP ([500 μ M]). % ΔV is the percentage reduction in velocity due to the ADP inhibition. Exp. Data = Experimental Data. N/M= Not measured. *According to our analysis (see Extended Experimental Procedure), the number of mutant subunits in the slowest population is 3 or 4.